

Sustained Bauxite Residue Rehabilitation with Gypsum and Organic Matter 16 years after Initial Treatment

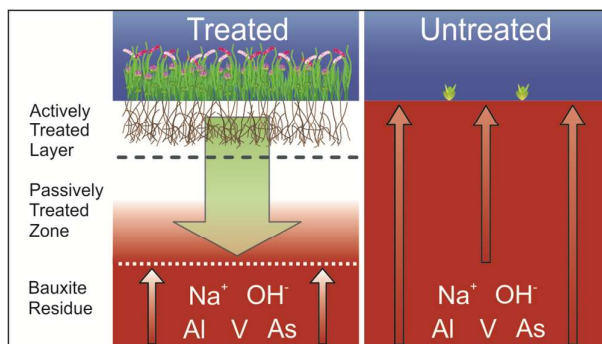
Andrew William Bray, Douglas I. Stewart, Ronan Courtney, Simon Rout, Paul N. Humphreys, William Matthew Mayes, and Ian T. Burke

Environ. Sci. Technol., **Just Accepted Manuscript** • DOI: 10.1021/acs.est.7b03568 • Publication Date (Web): 28 Nov 2017

Downloaded from <http://pubs.acs.org> on November 30, 2017

Just Accepted

“Just Accepted” manuscripts have been peer-reviewed and accepted for publication. They are posted online prior to technical editing, formatting for publication and author proofing. The American Chemical Society provides “Just Accepted” as a free service to the research community to expedite the dissemination of scientific material as soon as possible after acceptance. “Just Accepted” manuscripts appear in full in PDF format accompanied by an HTML abstract. “Just Accepted” manuscripts have been fully peer reviewed, but should not be considered the official version of record. They are accessible to all readers and citable by the Digital Object Identifier (DOI®). “Just Accepted” is an optional service offered to authors. Therefore, the “Just Accepted” Web site may not include all articles that will be published in the journal. After a manuscript is technically edited and formatted, it will be removed from the “Just Accepted” Web site and published as an ASAP article. Note that technical editing may introduce minor changes to the manuscript text and/or graphics which could affect content, and all legal disclaimers and ethical guidelines that apply to the journal pertain. ACS cannot be held responsible for errors or consequences arising from the use of information contained in these “Just Accepted” manuscripts.

21 **Graphical Abstract**

22

23

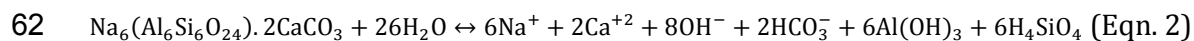
24 Abstract

25 Bauxite residue is a high volume by-product of alumina manufacture which is
26 commonly disposed of in purpose-built bauxite residue disposal areas (BRDAs). Natural
27 waters interacting with bauxite residue are characteristically highly alkaline, and have
28 elevated concentrations of Na, Al, and other trace metals. Rehabilitation of BRDAs is
29 therefore often costly and resource/infrastructure intensive. Data is presented from
30 three neighbouring plots of bauxite residue that was deposited twenty years ago. One
31 plot was amended 16 years ago with process sand, organic matter, gypsum, and seeded
32 (fully treated), another plot was amended 16 years ago with process sand, organic
33 matter, and seeded (partially treated), and a third plot was left untreated. These surface
34 treatments lower alkalinity and salinity, and thus produce a substrate more suitable for
35 biological colonisation from seeding. The reduction of pH leads to much lower Al, V and
36 As mobility in the actively treated residue and the beneficial effects of treatment extend
37 passively 20-30 cm below the depth of the original amendment. These positive
38 rehabilitation effects are maintained after 2 decades due to the presence of an active
39 and resilient biological community. This treatment may provide a lower cost solution to
40 BRDA end of use closure plans and orphaned BRDA rehabilitation.

41 Introduction

42 Globally, >100 million tonnes of alumina is produced annually.¹ Producing 1
43 tonne of alumina generates 1-2 tonnes of bauxite residue (known as “red mud”). The
44 residue varies with ore type, but all are alkaline, sodic, and contain similar minerals. In
45 the Bayer process bauxite ore is digested with NaOH at high temperature and pressure
46 which results in recrystallization of iron oxides present. Silica is a common impurity,
47 which is removed from solution by precipitation of a range of characteristic Na- and Ca-
48 aluminosilicate phases (e.g. sodalite and cancrinite).^{2,3} These “desilication products”
49 reside predominantly in the fine fraction. Residual aluminium (oxy)hydroxide phases,
50 quartz, zircon and titanium oxides (e.g. rutile and perovskite) also occur in the
51 residues.^{2,3}

52 Bauxite residue has few uses (cement, iron and steel production, construction
53 materials) and most is sent to bauxite residue disposal areas (BDRAs).⁴ The liquid from
54 bauxite residue is very alkaline (pH 11-13) and contains abundant sodium.⁵⁻⁷
55 Subsequent dissolution of desilication products such as sodalite (Eqn 1.) and cancrinite
56 (Eqn 2), along with associated amorphous secondary phases, generates further
57 alkalinity and releases sodium in the long term.⁸⁻¹⁰ Trace elements in bauxite, such as V
58 and As, become concentrated in the residue, and are often hosted in surface complexes
59 and secondary phases.¹⁰⁻¹⁴ This can be environmentally problematic as Al, V, and As
60 form aqueous oxyanions in alkaline conditions which sorb poorly to sediments^{15,16}.



63 When left untreated, bauxite residue is infiltrated by CO₂ and the formation of
64 aqueous and solid carbonate consumes OH⁻, lowering pH.¹⁷⁻¹⁹ The depth to which this
65 process can act within bauxite residue is controlled by the rate of in-gassing and
66 diffusion of CO₂. These process can be enhanced by gypsum addition, providing excess
67 Ca²⁺ for precipitation of carbonate.²⁰ These reactions occur rapidly at high pH and can
68 eventually buffer the pH to 7.5-8.5.^{17,21} Previous work has shown that gypsum addition
69 can also decrease the mobility of trace metals and Al in bauxite residue effected
70 soils.^{17,21} Other approaches to decrease bauxite residue salinity and alkalinity, such as
71 treatment with acid²² and seawater,²³ tend to only neutralise the aqueous, not the solid
72 alkalinity generating phases. Ion exchange resins,²⁴ and bipolar-membranes
73 electrodialysis²⁵ have been used to increase the longevity of treatment, yet these
74 approaches rely on continued management and the utilisation of products by an active
75 refinery. As such, common end-of-use practice is to cap BRDAs with an impermeable
76 layer, cover with topsoil, and revegetate. The costs “cap and cover” approaches are high
77 (e.g. 100k €/ha has been estimated for the BRDA in this study). However abandoning
78 BRDAs without surface cover may lead to problems with long term water infiltration
79 and dust formation.

80 Over the last 15 years Courtney and others have examined the effect of coarse
81 fraction bauxite residue (process sand), gypsum, and organic matter on the revegetation
82 of bauxite residue at Aughinish Alumina Refinery BRDA, Ireland.²⁶⁻³⁶ These studies have
83 assessed site rehabilitation by investigating macro- and microbiology, nutrient
84 availability, and the chemical nature of the substrate. Beneficial effects from bio-
85 rehabilitation have also been reported elsewhere.^{37,38} Yet, little is known of the
86 longevity and reliability of such surface treatments. Lack of long term data, and poorly

87 constrained audit trails regarding treatment and planting histories, can limit their
88 viability in BRDA closure plans. The objective of this study was to assess the long term
89 effects of a surface treatment to bauxite residue. Here we report the chemical and
90 mineralogical data sampled from depth profiles of bauxite residue nearly two decades
91 after initial treatment, and evaluate the ability of these treatments to provide sustained
92 rehabilitation of the substrate and associated fluid.

93 **Methods**

94 In September 2015 trial pits were dug to ~60 cm in a BRDA located in a
95 European Union member state with a temperate oceanic climate (average annual
96 rainfall ~1m). At this site bauxite residue was deposited into a 3m deep disposal cell in
97 1995, and subsequently treated to encourage revegetation in 1999. Therefore,
98 sampling was undertaken 20 years after deposition and 16 years after treatment.³¹
99 Three plots within the BRDA were investigated. The fully treated plot was amended
100 with gypsum (3% w/w rotavated-in to a depth 30 cm), process sand (10% w/w
101 rotavated-in to a depth of 30cm), spent mushroom compost (80t Ha⁻¹ rotavated-in to a
102 depth of 20cm), and seeded with a grassland mix (*Agrostis stolonifera*, *Holcus lanatus*,
103 *Lolium perenne*, *Trifolium repens*, and *Trifolium pratense*; 100 kg/ha).³¹ The partially
104 treated plot was amended only with process sand, spent mushroom compost, and then
105 seeded. The third plot was left untreated. Samples of bauxite residue were collected to a
106 depth of 50 cm from the trial pits in each of three different treatment zones. Duplicate
107 sample profiles in each plot were taken from two separate clean vertical surfaces of trial
108 pits and stored in polypropylene tubes. The dual depth profiles were sampled to
109 observe and account for heterogeneity in the residue.

110 Field moist samples were stored at 5 °C before aqueous extraction for major and
111 trace metals. 10 gram subsamples were mixed with 10 mL of ultrapure water (18.5 MΩ)
112 and shaken at room temperature for seven days. The solution pH was measured using a
113 Thermo Scientific Orion ROSS Ultra electrode calibrated with 4.00, 7.00, and 10.00
114 buffers (Fisher Scientific). 1 gram field moist subsamples were mixed with 10 mL of a
115 0.1 M Na₂HPO₄ in 0.01 M NaOH and shaken at room temperature for 7 days for
116 phosphate extraction of metal oxyanions. Supernatant solutions from both the water

117 and phosphate extractions were filtered through 0.2 μm disposable polyethersulfone
118 filters (Sartorius) and acidified in 5% HNO_3 for subsequent aqueous analysis by ICP-OES
119 (Thermo Fisher iCAP 7400 Radial ICP-OES) (see SI section S1 for further details).

120 Further 10 g field moist subsamples were also dried at 105 $^\circ\text{C}$ for 24 hours to
121 determine residue water content and for subsequent analysis by X-ray ray diffraction
122 (XRD; Bruker D8 Advance diffractometer, 12 min. scans, 2 to 70 $^\circ$ 2θ), X-ray fluorescence
123 (XRF, Olympus Innovex X-5000 XRF analyser) and total carbon analysis (TC; LECO SC-
124 144DR carbon analyser). The crystalline phases present were determined from XRD
125 patterns by peak fitting using EVA (version 3.0, Bruker), and semi-quantitative relative
126 proportions were calculated by Rietveld refinement using Topas (version 4.2, Bruker).
127 Total organic carbon (TOC) were measured after a 24 hour digestion in 10% HCl at
128 room temperature. Total inorganic carbon (TIC) was calculated from TC and TOC
129 measurements.

130 Acid soluble inorganic and organic substances (AIC and AOC) were determined
131 in 12 samples after extraction with 2 M HCl (1 g soil in 5 mL of 2 M HCl for 3 days at 4
132 $^\circ\text{C}$). The extractant was then separated by centrifugation at 8000 g for 10 min, pH
133 neutralised by drop-wise addition of 2 M NaOH, evaporated to dryness; and finally the
134 resulting solid dissolved in ultra-pure water at 1 $\text{g}\cdot\text{L}^{-1}$.³⁹ Total carbon and total
135 inorganic carbon in the extractant was determined using a Shimadzu total organic
136 carbon analyser 5050A (LOD 4 $\mu\text{g kg}^{-1}$).

137 Separate samples of bauxite residue were collected from beneath the exposed
138 vertical surface of each trial pit using a clean spatula, and sealed in sterile
139 polypropylene centrifuge tubes. These samples for DNA analysis were refrigerated
140 within 4 hours and frozen within 48hrs. DNA was isolated from 0.5 g of each sample

141 using the MPBio FastDNA SPIN Kit for Soil. Isolated DNA mass from each sample was
142 determined by Qubit dsDNA High Sensitivity assay on a Qubit Fluorometer (Life
143 Technologies; further details of quantification are in SI Section S3). DNA samples were
144 sent to the Centre for Genomic Research, University of Liverpool, where Illumina
145 TruSeq adapters and indices were attached to DNA fragments in a two-step PCR
146 amplification that targets the V4 hyper-variable region of the 16s rRNA gene,⁴⁰ and the
147 result was sequenced on the MiSeq platform. Reads were processed using the UPARSE
148 pipeline⁴¹ within the USEARCH software package (version 10, SI Section S3).⁴² Sequence
149 reads were allocated to operationally taxonomic units (OTUs) based on a minimum
150 sequence identity of 97% between the putative OTU members, and then classified using
151 the SILVA Living Tree Project 16s database, version 123.⁴³

152 Difference in average element concentration between plot treatments
153 (untreated, fully treated, and partially treated) was tested by ANCOVA (Analysis of Co-
154 Variance) using a general linear model to assess difference in average concentrations
155 across the treatments, with depth of sample as a co-variate. Pairwise comparisons were
156 tested by post-hoc Tukey test using a significance level of $p = 0.05$. Statistical
157 significance was expressed at $p < 0.05$ and $p < 0.001$ and the degrees of freedom for all
158 tests varied between 19 and 64.

159 **Results**

160 *Sampling observations*

161 Both the fully treated and partially treated sites were vegetated with a variety of
162 perennial grasses (*Holcus lanatus*), trifoliolate clovers (*Trifolium pratense*), and occasional
163 small shrubs (*Salix* spp.; Fig. S1), as has been described previously.³¹ The untreated plot
164 was largely unvegetated with one or two areas of stunted grasses (Fig. S1). The root
165 zone of the fully treated and partially treated sites extended approximately 15 cm
166 beneath the surface, and below 20cm the substrate had the appearance of dewatered
167 bauxite residue with little change in appearance to 50 cm depth. The untreated profile
168 had no root zone and at all depths had a very similar appearance to the residue in the
169 other profiles at depths below 20 cm. The bottom of the untreated pit filled with
170 leachate to a depth of about 10 cm after 2 hours.

171 *Substrate characteristics*

172 The pH of the untreated residue was 10.2 at the surface and steadily increased to
173 12.0 at a depth of 50 cm (Fig. 1; SI Table S2). The pH of the treated plots were notably
174 and significantly lower ($p < 0.001$; Table S3). The fully treated residue was pH 7.6 at the
175 surface, and increased steadily to a value of 9.6 at a depth of 50 cm. The pH value of the
176 partially treated residue was 7.6 at the surface, increased steadily to a value of 10.8 at a
177 depth of 50 cm, and was not significantly different from the fully treated residue ($p >$
178 0.05 ; Fig 2; Table S2-3).

179 The amount of sodium available to aqueous extraction of the untreated bauxite
180 residue was ~ 900 mg kg⁻¹ of bauxite residue, and with exception of concentrations at
181 the surface and at 50 cm there was little variation with depth (Fig. 1, Table S2). The

182 amount of Na that could be extracted from the fully treated and partially treated
183 samples demonstrated no trend with depth and were not significantly different from
184 each other ($p > 0.05$; Table S3). Fully and partially treated residue contained
185 concentrations approximately 10-15 % of those extracted from the untreated residue at
186 the same depth ($p < 0.001$; Fig. 1; Table S2-3). The concentration of silicon available to
187 aqueous extraction in the untreated bauxite residue was 5 mg kg^{-1} , and apart from the
188 measured concentration from 50 cm there was minimal variation with depth (Fig. 1,
189 Table S2). Si concentrations extracted from fully treated and partially treated bauxite
190 residue were $\sim 4 \text{ mg kg}^{-1}$ below 5 cm, and $\sim 13 \text{ mg kg}^{-1}$ above 5cm, there was no
191 significant difference between fully, partially, or untreated residue ($p > 0.05$; Fig. 1;
192 Table S2-3). Calcium concentrations from the aqueous extraction of untreated bauxite
193 residue ranged from 3 mg kg^{-1} at the surface to below the limit of detection at 50 cm
194 (0.11 mg kg^{-1}) (Fig. 1, Table S2). In contrast Ca concentrations from fully treated and
195 partially treated samples were significantly different to the untreated residue ($p <$
196 0.001 ; Table S3), 143 mg kg^{-1} at the surface decreasing to $\sim 10 \text{ mg kg}^{-1}$ at 20 cm, with
197 further slight concentration decrease to $\sim 2 \text{ mg kg}^{-1}$ at 50 cm with no significant
198 difference between treatments ($p > 0.005$; Fig. 1; Table S2-3).

199 The aluminium concentration available to aqueous extraction in untreated
200 bauxite residue was $\sim 10 \text{ mg kg}^{-1}$ at the surface which increases steadily with depth to
201 $\sim 65 \text{ mg kg}^{-1}$ at 50 cm (Fig 2. Table S2). Conversely, Al concentrations available in fully
202 and partially treated samples were significantly different ($p < 0.001$, Table S3) and near
203 the detection limit (0.09 mg kg^{-1}) at all depths, apart from at 30-50 cm where Al
204 concentrations were $1-10 \text{ mg kg}^{-1}$ (Fig 2. Table S2). There was no significant difference
205 between treatments ($p > 0.05$, Table S3). The amount of vanadium available to aqueous

206 extraction from untreated bauxite residue was $\sim 5 \text{ mg kg}^{-1}$ and did not vary greatly with
207 depth (Fig 2. Table S2). Aqueous extractable V in fully treated and partially treated
208 samples were near detection limit at the surface (0.03 mg kg^{-1}) and increased gradually
209 with depth to maximum concentrations of 3.9 mg kg^{-1} at 50 cm, significantly different
210 from untreated residue ($p < 0.001$, Table S3) but not significantly different between
211 fully and partially treated residue ($p > 0.05$; Fig 2; Table S2-3). Aqueous available
212 arsenic concentrations from untreated bauxite residue were highest at the surface (0.3
213 mg kg^{-1}) and decrease with depth to 0.9 mg kg^{-1} at 50 cm depth (Fig 2. Table S2). With
214 the exception of one sample, all measurements of aqueous extractable As from fully
215 treated and partially treated bauxite residue were below detection limit (0.045 mg kg^{-1})
216 and significantly different from the untreated residue ($p < 0.001$; Fig 2; Table S2-3).
217 Extraction at high pH using disodium phosphate demonstrated substantial
218 concentrations of Al, V, and As were available in all bauxite residue treatments.
219 Phosphate extractable Al concentrations from all treatments are generally all $25\text{-}50 \text{ mg}$
220 kg^{-1} at all depths (no significant differences between treatments; $p > 0.05$; Table S2-3). V
221 concentrations from the phosphate extraction of untreated bauxite residue range from
222 $30\text{-}75 \text{ mg kg}^{-1}$ at the surface to 30 mg kg^{-1} at 50 cm depth (Fig 2. Table S2). Phosphate
223 available V from fully treated and partially treated samples was lowest at the surface
224 ($\sim 15 \text{ mg kg}^{-1}$) and increases with depth to $\sim 75 \text{ mg kg}^{-1}$ at 50 cm, but with no significant
225 differences between untreated, fully treated, or partially treated residue ($p > 0.05$; Fig 2.
226 Table S2-3). Arsenic concentrations extracted from untreated bauxite residue at high
227 pH with phosphate are $\sim 2.5 \text{ mg kg}^{-1}$ at the surface and decrease to $< 1 \text{ mg kg}^{-1}$ at 50 cm
228 (Fig 2. Table S2). Phosphate extractable As from fully treated and partially treated
229 samples increase with depth from $\sim 1 \text{ mg kg}^{-1}$ at the surface to $\sim 2.5 \text{ mg kg}^{-1}$ at 50 cm
230 (Fig 2. Table S2). Phosphate extractable As from fully treated and partially treated

231 residue were significantly different ($p < 0.05$), though neither were significantly
232 different from the untreated residue ($p > 0.05$; Table S3).

233 The water content of the residue (weight of water as % of dry weight) at both the
234 fully and partially treated sites was over 50% near the surface, exhibited a minimum of
235 ~30 % at approximately 10 cm, and then increased to between 35 and 45 % at depths
236 below 20 cm (Table S2). In contrast the water content in the untreated profile was 35%
237 near to the surface, exhibited a maximum value of ~50 % at 10cm, and then decreased
238 slightly to 40 % at depths below 30 cm. Water in the untreated residue was significantly
239 different to fully treated residue ($p < 0.001$), but not significantly different from
240 partially treated residue ($p > 0.05$; Table S3)

241 The bulk mineralogy of bauxite residue from all plots were largely similar and
242 consist of 40-45% iron oxy-hydroxides, 20-30% aluminium oxy-hydroxides, 20-30%
243 titanium oxides, and 10-15% feldspathoids (Table 1, Table S4). At the untreated bauxite
244 residue plot there were no differences in the relative proportions of each phase with
245 depth. Variations in the relative proportions of phases within the residue as a function
246 of depth and treatment were within the range of uncertainty of Rietveld refinement (5
247 %). The alkali generating feldspathoid and desilication product cancrinite was present
248 at all depths in all treatment sites (Table 1, Table S4). There was little difference in the
249 bulk elemental composition measured by XRF with either depth or treatment (Table
250 S5). Fe, Al, Ca, Si and Ti were the most abundant oxides in present each site (36 ± 3 ,
251 10 ± 2 , 15 ± 2 , 5 ± 1 and 4 ± 1 wt. % respectively). Carbon was most concentrated in the
252 top 10 cm of the fully treated profile (Fig. 3), where TOC was approximately 2.5% and
253 TIC was 1.5%. Below 10 cm there was no discernible difference in carbon content
254 between the fully treated and untreated profiles. Samples of untreated bauxite had less

255 than 0.5% TOC and TIC at all depths. Acid extractable inorganic carbon (AIC) and
256 organic carbon (AOC) was only detectable in the top 10 cm of the fully treated and
257 untreated bauxite residue, and was below or at the limit of detection ($<4 \mu\text{g kg}^{-1}$) in all
258 other samples (Table S2).

259 DNA mass isolated per gram of sample demonstrated a strong vertical gradient
260 and significant difference between the treated (fully treated and partially treated) and
261 untreated sites (Fig. 3, Table S6). DNA was concentrated in the top 12 cm of the fully
262 treated and partially treated sites where maximum concentrations were up to $14.3 \mu\text{g g}^{-1}$.
263 The highest concentration of DNA in the untreated samples was $2.3 \mu\text{g g}^{-1}$ in the near
264 surface. Below 12 cm the DNA concentrations in the fully treated, partially treated and
265 untreated residue were negligible.

266 Sufficient bacterial DNA was recovered from the fully treated substrate (2 cm),
267 and partially treated substrate (2 and 5 cm) for Next Generation Sequencing (DNA
268 recovery from the untreated substrate was insufficient). Nine phyla individually
269 represented more the 1% of the population of each sample (Fig. S2, Table S7). At this
270 taxonomic level, there was little difference between bacterial communities of the fully
271 treated and partially treated substrate, with the most abundant phyla being
272 Acidobacteria (37 % of reads), Actinobacteria (19 %), Proteobacteria (18 %), and
273 Planctomycetes (14 %). The most abundant class within the Acidobacteria phylum was
274 Acidobacteria Gp6 (48 % of Acidobacteria). Actinomycetales (74 %) was the most
275 abundant order within the Actinobacteria phylum. Alphaproteobacteria (67 %) was the
276 most abundant class within the Proteobacteria. 100 % of the Planctomycetes phylum
277 mapped onto the Planctomycetaceae family.

278 The alpha diversity indices for each sample are shown in Table S8. Here we use
279 Hill numbers^{44,45} as robust bacterial diversity measures which account for the
280 distortions of rare taxa.⁴⁴⁻⁴⁷ D_0^α , the operational taxonomic unit (OTU) richness, ranges
281 from ~1250 to 3850, however this diversity index is very sensitive to rare taxa, and
282 takes no account of OTU relative abundance. Indices that give a measure of the number
283 of common (D_1^α) and dominant OTUs (D_2^α ; Table S8), converge across the samples,
284 demonstrating similar diversity in the OTU populations. Common OTUs represent >79
285 % of total sequence reads in each sample, and dominant OTUs accounted for 51-62 % of
286 total reads in each sample.

287

288 Discussion

289 *The geochemistry of 20 year old untreated bauxite residue*

290 Fresh bauxite residue is highly alkaline (pH 10–13), highly sodic (abundant
291 mobile Na), contains abundant solid phase alkalinity (e.g. desalination products; 2-51%)
292 and can also contain trace metals above threshold intervention levels.^{10,12,26,27,48–52}
293 The desilication products in fresh residue tend to have higher proportion of sodalite to
294 cancrinite¹⁰ however, with age sodalite can transform into cancrinite.⁵³ Initially the high
295 pH and sodium contents are due to remnant NaOH from the Bayer Process. Previous
296 work has shown that repeated replacement of pore water decreases the mass of fresh
297 bauxite residue but does not alter final pH, Na⁺, Al(OH)₄⁻, CO₃²⁻, or OH⁻ concentrations⁸
298 due to the dissolution desilication products, and associated amorphous phases (Eqn 1,
299 2). When left untreated, the pH of bauxite residue is controlled by the balance between
300 CO₂ infiltration from the atmosphere, and OH⁻ production through desilication product
301 dissolution.

302 20 years after deposition the measured pH of the untreated bauxite residue
303 ranges from pH 10 at the surface to pH 12 at 50 cm. XRD analysis indicates that
304 cancrinite was the primary desilication product present (Table S4). At the surface, CO₂
305 in-gassing, in combination with cancrinite dissolution, and associated amorphous Fe, Al,
306 and Si phase solubility, buffers the pore fluids to approximately pH 10. Atmospheric CO₂
307 in-gassing appears to extend ~20 cm from the surface (Fig. 1). Below 20 cm the bauxite
308 residue appears to be isolated from the atmosphere and dissolution of cancrinite results
309 in higher pH (≥ 11.5 ; Fig. 1). Cancrinite dissolution also controls long term Na
310 availability (Eqn. 2), and results in aqueous available Na concentrations of ~ 900 mg kg⁻¹
311 in untreated bauxite residue after 20 years. However, dissolution of cancrinite appears

312 to be incongruent at high pH. Cancrinite dissolution should produce equimolar
313 concentrations of Na, Si, and Al, (Eqn. 2) but the measured concentrations are far from
314 stoichiometric (Fig. S3). Aqueous extractable Na concentrations from untreated samples
315 are 100 to 400 times higher in concentration than extractable Si and 10 to 150 times the
316 Al concentration, indicating a preferential retention of Si and Al in the solid phase.

317 This preferential retention of Al and Si in the solid phase is probably controlled
318 by the precipitation of amorphous and crystalline secondary phases. At the highest pH
319 measured, Al concentrations are close to equilibrium with gibbsite ($\text{Al}(\text{OH})_3$) (Fig S3).
320 The measured Al concentrations decrease as the pH decreases from 12 to 10, but
321 exceeds concentrations in equilibrium with gibbsite. Over this pH range, Si
322 concentrations are much lower than those expected for $\text{SiO}_{2(\text{am})}$ equilibrium, suggesting
323 an alternative solubility limiting phase. At high pH, with high Na concentrations, Al and
324 Si can co-precipitate in amorphous cation-bridged alumino-silicate gels,⁵⁴ which may
325 explain the low concentrations observed.

326 Sustained alkalinity generation throughout untreated bauxite residue is a
327 concern because it may be associated with increased mobility of potentially toxic
328 metal(oid) oxyanions such as Al, V, and As. Both V and As are reported to be present in
329 bauxite residues primarily in the 5+ oxidation state as vanadate and arsenate species
330 ^{10,12}, and are found as surface adsorbed species (V can also be associated with
331 neoformed hydrogarnet phases such as Katoite).¹² Conversely, Al availability is usually
332 controlled by the solubility of Al (oxy)hydroxide phases, which typically have much
333 higher solubility at high pH (see discussion above).⁵⁵ In alkaline phosphate extractions
334 both OH^- and phosphate ions compete strongly for available sorption sites and promote
335 the mobility of metal oxyanions.^{14,20} The results of these extractions, therefore,

336 demonstrate that there is abundant V and As adsorbed to bauxite residue (Fig. 2). In the
337 untreated samples, where $\text{pH} > 10$, As and V sorb poorly to mineral surfaces,^{14-16,21,56-58}
338 which is why only 10 and 15 % of the phosphate extractable As and V respectively were
339 extractable water this fraction will be mobile in residue pore waters.

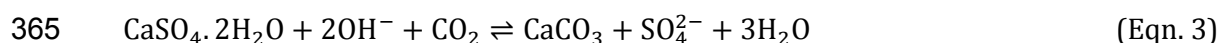
340 In summary, the bauxite residue from the untreated plot retains many of the
341 characteristics of the fresh bauxite residue 20 years after deposition: high pH, a sizeable
342 quantity of desilication products (particularly cancrinite), abundant available Na, high
343 Al, V, and As concentrations, low organic carbon concentrations. Thus, untreated, it is an
344 environment that is not conducive to spontaneous macro- or microorganism
345 colonization through translocation.

346

347 *Treated bauxite residue*

348 16 years after bauxite residue treatment with process sand, organic matter and
349 gypsum significant pH reduction (2 units) was observed over a depth that extends at
350 least 30 cm below the actively treated surface layer (Fig. 1; Table S2). Aqueous sodium
351 concentrations were an order of magnitude lower in the treated plots than untreated
352 plot at all depths (Fig. 1; Table S2), and the availability of aluminium, vanadium, and
353 arsenic were all lower in treated than untreated bauxite residue (Fig. 2; Table S2).
354 These observations demonstrate that positive treatment effects observed in the short
355 term are sustained, such as: improved permeability, particle aggregation, and drainage;
356 pH neutralisation; decreased Na, Al, and Fe availability.^{28,29} In natural soils, organic
357 matter plays a key role in controlling particle aggregation,⁵⁹⁻⁶¹ and the application of
358 spent mushroom compost may have improved residue structure. In highly alkaline

359 conditions, organic matter dissolves and hydrolyses to form humic substances and
360 lower molecular weight organic anions.⁶²⁻⁶⁴ This process lowers pH and releases
361 organic bound nutrients to the local environment. Other studies have reported
362 significant reduction in pH following organic matter application to bauxite
363 residue.^{28,29,65,66} Gypsum application enhances pH neutralisation by CO₂ in-gassing via
364 the precipitation of CaCO₃.^{20,21} The net reaction for this mechanism is:



366 Increased CO₂ in-gassing and formation of dissolved carbonate species (supplementary
367 information Eqns S2-7) can buffer the pH to 7.5-8, similar to natural alkaline soils, thus
368 producing an environment less hostile to biological colonisation. At this site bauxite
369 residue treatment with gypsum (in addition to process sand and organic matter)
370 resulted in greater plant biomass in the first two years of growth,²⁶⁻²⁸ and a more
371 diverse and developed vegetation succession after 6 years (i.e. partial replacement of
372 clover by more extensive grass cover and the establishment of small shrubs).³¹
373 However, 16 years after treatment, there is no significant chemical or microbiological
374 difference between the fully and partially treated substrate.

375 Long term alkalinity generation and sodium release in the 20 year old bauxite
376 residue is controlled by cancrinite dissolution. Cancrinite dissolution kinetics as a
377 function of pH is unreported in the literature, but the feldspathoids leucite and
378 nepheline exhibit dissolution kinetics that decrease by an order of magnitude as pH
379 decreases from 12 to 7.⁶⁷⁻⁷⁰ The dissolution kinetics of multioxide silicates, including
380 aluminosilicates, are controlled by the solubilities of secondary phases,⁷¹ thus it is
381 inferred that these decreases in feldspathoid dissolution rate are linked to the
382 solubilities of secondary aluminium and silicon phases. It is reasonable to expect

383 cancrinite dissolution kinetics to vary with pH in a similar manner to other
384 feldspathoids, decreasing by an order of magnitude between pH 12 and 7. This suggests
385 pH conditions established in treated bauxite residue from organic matter and gypsum
386 addition decrease the rate of OH^- and Na^+ production from the dissolution of cancrinite
387 and associated secondary phases (Fig. 1).

388 Aqueous extracted aluminium concentrations from partially and fully treated
389 bauxite residue plotted as a function of pH (Fig. S3) fall on a line parallel to, but in
390 between, the solubility lines of gibbsite and $\text{Al}(\text{OH})_3$ (am). This is different to the trend
391 observed for the untreated samples at higher pH, suggesting a different solubility
392 controlling phase. Between pH 8 and 10 formation of dawsonite ($\text{NaAlCO}_3(\text{OH})_2$) and an
393 amorphous precursor to boehmite have been observed in bauxite residue
394 treatment.^{12,72} and may be the solubility controlling phases at this site. The phosphate
395 extraction shows that there is abundant extractable Al, V, and As in both the partially
396 and fully treated bauxite residue (Fig. 2; Table S2). However the aqueous extractions
397 showed that nearer to neutral pH Al is secured in secondary phases, and the majority of
398 V and As is sorbed to mineral surfaces^{14-16,21,56-58} making Al, V, and As, much less
399 available to aqueous solution (Fig. 2).

400

401 *Long term maintenance of beneficial conditions*

402 Rehabilitation of bauxite residue disposal areas by vegetation using the
403 treatments described here is a pH dependant processes with benefits extending 20-30
404 cm beyond the initial treatment depth. After 20 years of rainwater infiltration the
405 alkalinity generating phases have not been exhausted, thus other processes must be

406 controlling residue neutralisation. 16 years after treatment, the original additives are
407 largely unobservable, with little chemical difference remaining from the application of
408 gypsum. This suggests that the development of resilient vegetation on bauxite residue,
409 along with associated rhizosphere microorganisms, may drive long term stability and
410 chemical safety of treated bauxite residue. The organic matter applied to the surface
411 layers is only detected in small quantities (Fig. 3) and has likely been degraded and
412 recycled into plants and microorganisms. The products of gypsum addition are minimal;
413 calcite was undetectable by XRD, and there is only a slight accumulation of Ca and TIC
414 towards the surface of both treated zones. Process sand was present in the surface layer
415 when sampling but heterogeneously distributed and undetectable mineralogically by
416 XRD and chemically by XRF.

417 The supply of H⁺ ions to depth that is driving pH neutralisation in treated bauxite
418 residue may be photosynthetic in origin. This can occur via a combination of three
419 mechanisms: (a) enhanced CO₂ flux from plant roots and associated microorganism
420 respiration; (b) organic matter degradation in the biologically active surface layer,
421 producing low molecular weight organic acids; and (c) secretion of low molecular
422 weight organic acids by plant roots and rhizospheric microorganisms. The carbon flux
423 from atmosphere to rhizosphere is well documented in both the short (i.e. respiration),
424 and medium terms (organic matter production).⁷³ Quantification of extracted DNA from
425 both the treated plots suggests a zone of greater biological activity in the top 12 cm of
426 treated bauxite residue (Fig. 3). DNA recovery is media dependent, with particle size
427 and pH potentially affecting the efficiency of extraction. This uncertainty may over
428 emphasise the gradient of biological activity with depth, and between treated and
429 untreated samples. The extracted DNA concentrations from the top 12 cm of treated

430 bauxite residue are within the range of extracted DNA concentrations from natural soils
431 (very approximate soil DNA concentrations range from 2.5 to 26.9 $\mu\text{g g}^{-1}$).⁷⁴ DNA
432 recovery from this site's untreated bauxite residue was insufficient for Next-Generation
433 Sequencing, however other workers have shown bauxite residue to contain alkali
434 tolerant bacteria.⁷⁵ Sequenced DNA recovered from the root zone substrate of the fully
435 and partially treated bauxite residue was dominated by the phyla Acidobacteria,
436 Actinobacteria, Proteobacteria, and Planctomycetes. Natural soil root zone or
437 rhizosphere bacterial communities frequently contain Actinobacteria, Bacteroidetes,
438 Firmicutes, and Proteobacteria taxa,⁷⁶⁻⁷⁸ which, with the exception of Firmicutes, are
439 present in our treated bauxite residue (Figure S2, Table S7). Many taxa of Acidobacteria
440 are known to be tolerant to high pH, and show increasing relative abundance with
441 increasing pH from 5.5 pH.⁷⁹⁻⁸² Many Planctomycetes taxa are halotolerant,⁸³⁻⁸⁷ existing
442 in freshwater, marine, and brackish environments. The presence of these phyla suggests
443 the microbial communities in the fully and partially treated bauxite residue are in
444 transition between a highly alkaline and saline residue microbiome, and a plant
445 supported subsurface microbiome.

446 Surface treatment with process sand, gypsum, and organic matter is a stable,
447 reliable, and safe solution to bauxite residue rehabilitation. Bauxite residue pH is
448 neutralised, Na^+ is less available, and metal oxyanions (Al, V, and As) are less mobile.
449 The beneficial effects of treatment are long term and extend 20-30 cm beyond the depth
450 of application. The formation a passively treated zone, which is $\geq 20\%$ of the total
451 disposal cell depth, is sufficient to separate the surface environments from the
452 potentially highly alkaline, sodium rich, and trace metal containing residue at depth.
453 The presence of alkalinity generating phases in both treated plots highlights the

454 importance of maintaining a strong biologically active surface layer. Were this layer to
455 be removed or substantially disrupted, and its supply of acid neutralising molecules
456 lost, the system would likely return to a high pH steady state, with high Na, Al, V, and As
457 concentrations, similar to those observed in the untreated bauxite residue.

458 This is the first observation of a shallow surface layer of actively treated and
459 vegetated residue producing passive positive rehabilitation effects into deeper layers.
460 This rehabilitation is likely driven by biology activity at the surface and continues long
461 after the original treatment constituents (gypsum, organic matter) have been depleted.
462 Rehabilitation has resulted in a physical separation between deeper zones within the
463 residue (potentially containing high alkalinity, sodium, and trace metals) and the
464 bottom of the rooted zone at around 20 cm. Rehabilitation decreases the likelihood of
465 plants being exposed to the negative characteristics of bauxite residue, and lowers the
466 possibility of trace metal transfer into foliage and the wider ecosystem. The benefits of
467 this surface treatment extend beyond the environmental; the cost of application is
468 approximately 10k €/ha, whereas the cap and cover estimate for this BDRA is 100k
469 €/ha. Gypsum application accounts for approximately 50-70 % of the total treatment
470 cost, and assessment of its value for long term rehabilitation is important. Our results
471 suggest the development of a healthy vegetation cover is key to long term stability of
472 residue rehabilitation and previous work has demonstrated the role of gypsum in
473 rapidly, and successfully establishing a resilient vegetation layer.^{26-28,31,32,35} Gypsum
474 application may, therefore, offer additional security in vegetation establishment, and
475 the ultimate success and longevity of rehabilitation. However, 16 years after application
476 there are no significant chemical benefits from gypsum addition. Our study
477 demonstrates surface amendment of this nature is a viable closure option for active

478 BRDAs and a particularly good choice for rehabilitation of orphan sites where there is
479 an acute need to protect the public and environment at the lowest possible costs.

480 **Supporting Information**

481 Detailed aqueous analysis, DNA extraction, quantification, and post sequence processing
482 methods. Stepwise reactions of gypsum promoted CaCO_3 precipitation and pH
483 neutralisation. On site photographs of the trial pits. Additional figures of bacterial
484 community composition and elemental ratios and solubility. Additional tables with full
485 analytical results. Sequence reads have been uploaded to the National Center for
486 Biotechnology Information (NCBI) under the Sequence Read Archive (SRA) accession
487 number TBC. Collectively, the paper and these sources provide all the relevant data for
488 this study.

489 **Acknowledgements**

490 This research was funded by grant NE/L01405X/1 as part of the Resource
491 Recovery from Waste programme administered by the Natural Environment Research
492 Council (NERC), UK. The authors would like to thank Andy Connelly, Lesley Neve,
493 Stephen Reid, Sheena Bennett, and David Elliott at the University of Leeds for technical
494 support.

495

496 **References**

- 497 (1) World Aluminium. World Aluminium — Alumina Production [http://www.world-](http://www.world-aluminium.org/statistics/alumina-production/)
498 [aluminium.org/statistics/alumina-production/](http://www.world-aluminium.org/statistics/alumina-production/) (accessed May 26, 2017).
- 499 (2) Snars, K.; Gilkes, R. J. Evaluation of bauxite residues (red muds) of different
500 origins for environmental applications. *Appl. Clay Sci.* **2009**, *46* (1), 13–20.
- 501 (3) International Aluminium Institute. *Bauxite Residue Management: Best Practice*
502 www.european-aluminium.com; 2015.
- 503 (4) Power, G.; Gräfe, M.; Klauber, C. Bauxite residue issues: I. Current management,
504 disposal and storage practices. *Hydrometallurgy* **2011**, *108* (1), 33–45.
- 505 (5) Hind, A. R.; Bhargava, S. K.; Grocott, S. C. The surface chemistry of Bayer process
506 solids: a review. *Colloids Surfaces A Physicochem. Eng. Asp.* **1999**, *146* (1), 359–
507 374.
- 508 (6) Czop, M.; Motyka, J.; Sracek, O.; Szuwarzyński, M. Geochemistry of the
509 Hyperalkaline Gorka Pit Lake (pH > 13) in the Chrzanow Region, Southern
510 Poland. *Water, Air, Soil Pollut.* **2011**, *214* (1–4), 423–434.
- 511 (7) Mayes, W. M.; Jarvis, A. P.; Burke, I. T.; Walton, M.; Feigl, V.; Klebercz, O.; Gruiz, K.
512 Dispersal and Attenuation of Trace Contaminants Downstream of the Ajka
513 Bauxite Residue (Red Mud) Depository Failure, Hungary. *Environ. Sci. Technol.*
514 **2011**, *45* (12), 5147–5155.
- 515 (8) Thornber, M.; Binet, D. Caustic Soda Adsorption on Bayer Residues. In *5th*
516 *International Alumina Quality Workshop*; Alumina Worsley, Ed.; Bunbury, AQW
517 Inc., 1999; pp 498–507.
- 518 (9) Menzies, N. W.; Fulton, I. M.; Kopittke, R. A.; Kopittke, P. M. Fresh Water Leaching
519 of Alkaline Bauxite Residue after Sea Water Neutralization. *J. Environ. Qual.* **2009**,
520 *38* (5), 2050.
- 521 (10) Gräfe, M.; Power, G.; Klauber, C. Bauxite residue issues: III. Alkalinity and
522 associated chemistry. *Hydrometallurgy* **2011**, *108* (1), 60–79.
- 523 (11) Brunori, C.; Cremisini, C.; Massanisso, P.; Pinto, V.; Torricelli, L. Reuse of a treated
524 red mud bauxite waste: studies on environmental compatibility. *J. Hazard. Mater.*
525 **2005**, *117* (1), 55–63.
- 526 (12) Burke, I. T.; Mayes, W. M.; Peacock, C. L.; Brown, A. P.; Jarvis, A. P.; Gruiz, K.
527 Speciation of arsenic, chromium, and vanadium in red mud samples from the Ajka
528 spill site, Hungary. *Environ. Sci. Technol.* **2012**, *46*, 3085–3092.
- 529 (13) Klebercz, O.; Mayes, W. M.; Anton, Á. D.; Feigl, V.; Jarvis, A. P.; Gruiz, K.; Mander, Ü.;
530 Csákberényi-Malasics, D.; Tóth, Á.; Czitrovsky, A.; et al. Ecotoxicity of fluvial
531 sediments downstream of the Ajka red mud spill, Hungary. *J. Environ. Monit.*
532 **2012**, *14* (8), 2063.
- 533 (14) Lockwood, C. L.; Mortimer, R. J. G.; Stewart, D. I.; Mayes, W. M.; Peacock, C. L.;
534 Polya, D. A.; Lythgoe, P. R.; Lehoux, A. P.; Gruiz, K.; Burke, I. T. Mobilisation of
535 arsenic from bauxite residue (red mud) affected soils: Effect of pH and redox
536 conditions. *Appl. Geochemistry* **2014**, *51*, 268–277.
- 537 (15) Peacock, C. L.; Sherman, D. M. Vanadium(V) adsorption onto goethite (α -FeOOH)
538 at pH 1.5 to 12: a surface complexation model based on ab initio molecular
539 geometries and EXAFS spectroscopy. *Geochim. Cosmochim. Acta* **2004**, *68* (8),
540 1723–1733.
- 541 (16) Mamindy-Pajany, Y.; Hurel, C.; Marmier, N.; Roméo, M. Arsenic adsorption onto
542 hematite and goethite. *Comptes Rendus Chim.* **2009**, *12* (8), 876–881.

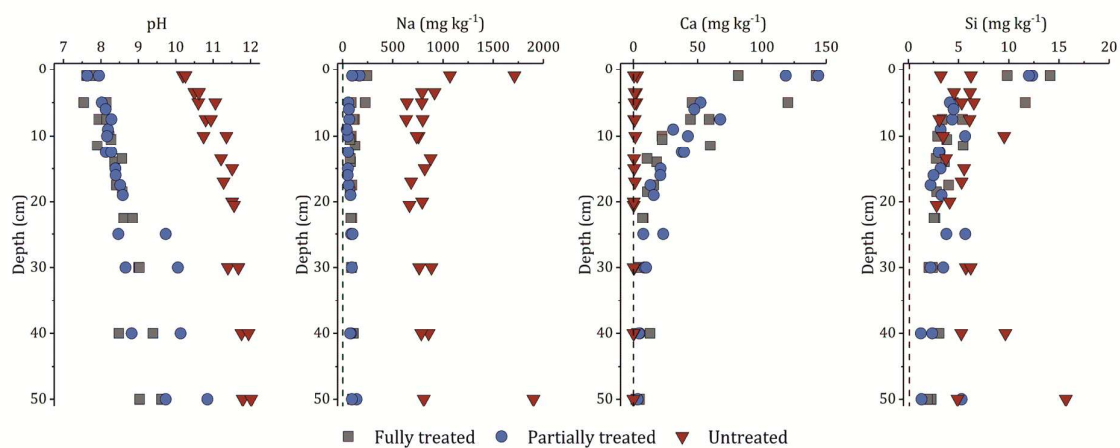
- 543 (17) Renforth, P.; Mayes, W. M.; Jarvis, A. P.; Burke, I. T.; Manning, D. A. C.; Gruiz, K.
544 Contaminant mobility and carbon sequestration downstream of the Ajka
545 (Hungary) red mud spill: The effects of gypsum dosing. *Sci. Total Environ.* **2012**,
546 *421*, 253–259.
- 547 (18) Alcoa. *Pinjarra Refinery Long Term Residue Management Strategy*; 2011.
- 548 (19) Alcoa. *Kwinana Refinery Long Term Residue Management Strategy*; 2012.
- 549 (20) Burke, I. T.; Peacock, C. L.; Lockwood, C. L.; Stewart, D. I.; Mortimer, R. J. G.; Ward,
550 M. B.; Renforth, P.; Gruiz, K.; Mayes, W. M. Behavior of Aluminum, Arsenic, and
551 Vanadium during the Neutralization of Red Mud Leachate by HCl, Gypsum, or
552 Seawater. *Environ. Sci. Technol.* **2013**, *47* (12), 6527–6535.
- 553 (21) Lehoux, A. P.; Lockwood, C. L.; Mayes, W. M.; Stewart, D. I.; Mortimer, R. J. G.; Gruiz,
554 K.; Burke, I. T. Gypsum addition to soils contaminated by red mud: implications
555 for aluminium, arsenic, molybdenum and vanadium solubility. *Environ. Geochem.*
556 *Health* **2013**, *35* (5), 643–656.
- 557 (22) Kirwan, L. J.; Hartshorn, A.; McMonagle, J. B.; Fleming, L.; Funnell, D. Chemistry of
558 bauxite residue neutralisation and aspects to implementation. *Int. J. Miner.*
559 *Process.* **2013**, *119*, 40–50.
- 560 (23) Hanahan, C.; McConchie, D.; Pohl, J.; Creelman, R.; Clark, M.; Stocksiek, C.
561 Chemistry of Seawater Neutralization of Bauxite Refinery Residues (Red Mud).
562 *Environ. Eng. Sci.* **2004**, *21* (2), 125–138.
- 563 (24) Wightman, G.; Davy Mckee Limited. Process for the removal of sodium values
564 from sodium contaminated solids. CA 2132638 A1, 1994.
- 565 (25) Kishida, M.; Harato, T.; Tokoro, C.; Owada, S. In situ remediation of bauxite residue
566 by sulfuric acid leaching and bipolar-membrane electro dialysis. *Hydrometallurgy*
567 **2016**.
- 568 (26) Courtney, R.; Timpson, J. P.; Grennan, E. Growth of *Trifolium pratense* in Red Mud
569 Amended With Process Sand, Gypsum and Thermally Dried Sewage Sludge. *Int. J.*
570 *Surf. Mining, Reclam. Environ.* **2003**, *17* (4), 227–233.
- 571 (27) Courtney, R. G.; Timpson, J. P. Nutrient status of vegetation grown in alkaline
572 bauxite processing residue amended with gypsum and thermally dried sewage
573 sludge - A two year field study. *Plant Soil* **2004**, *266* (1–2), 187–194.
- 574 (28) Courtney, R. G.; Timpson, J. P. Reclamation of Fine Fraction Bauxite Processing
575 Residue (Red Mud) Amended with Coarse Fraction Residue and Gypsum. *Water.*
576 *Air. Soil Pollut.* **2005**, *164* (1–4), 91–102.
- 577 (29) Courtney, R. G.; Jordan, S. N.; Harrington, T. Physico-chemical changes in bauxite
578 residue following application of spent mushroom compost and gypsum. *L. Degrad.*
579 *Dev.* **2009**, *20* (5), 572–581.
- 580 (30) Courtney, R.; Mullen, G. Use of Germination and Seedling Performance Bioassays
581 for Assessing Revegetation Strategies on Bauxite Residue. *Water. Air. Soil Pollut.*
582 **2009**, *197* (1–4), 15–22.
- 583 (31) Courtney, R.; Mullen, G.; Harrington, T. An evaluation of revegetation success on
584 bauxite residue. *Restor. Ecol.* **2009**, *17* (3), 350–358.
- 585 (32) Courtney, R.; Harrington, T. Growth and nutrition of *Holcus lanatus* in bauxite
586 residue amended with combinations of spent mushroom compost and gypsum. *L.*
587 *Degrad. Dev.* **2012**, *23* (2), 144–149.
- 588 (33) Courtney, R.; Kirwan, L. Gypsum amendment of alkaline bauxite residue – Plant
589 available aluminium and implications for grassland restoration - ScienceDirect.
590 *Ecol. Eng.* **2012**, *42*, 279–282.
- 591 (34) Schmalenberger, A.; O’Sullivan, O.; Gahan, J.; Cotter, P. D.; Courtney, R. Bacterial

- 592 Communities Established in Bauxite Residues with Different Restoration
593 Histories. *Environ. Sci. Technol.* **2013**, *47* (13), 7110–7119.
- 594 (35) Courtney, R.; Feeney, E.; O’Grady, A. An ecological assessment of rehabilitated
595 bauxite residue. *Ecol. Eng.* **2014**, *73*, 373–379.
- 596 (36) Courtney, R.; Harris, J. A.; Pawlett, M. Microbial Community Composition in a
597 Rehabilitated Bauxite Residue Disposal Area: A Case Study for Improving
598 Microbial Community Composition. *Restor. Ecol.* **2014**, *22* (6), 798–805.
- 599 (37) Santini, T. C.; Kerr, J. L.; Warren, L. A. Microbially-driven strategies for
600 bioremediation of bauxite residue. *J. Hazard. Mater.* **2015**, *293*, 131–157.
- 601 (38) Zhu, F.; Li, X.; Xue, S.; Hartley, W.; Wu, C.; Han, F. Natural plant colonization
602 improves the physical condition of bauxite residue over time. *Environ. Sci. Pollut.*
603 *Res.* **2016**, *23* (22), 22897–22905.
- 604 (39) Eaton, A. D.; Clesceri, L. S.; Rice, E. W.; Greenberg, A. E. *Standard Methods for the*
605 *Examination of Water & Wastewater*, 21st ed.; American Public Health
606 Association: Washington, DC, 2005.
- 607 (40) Caporaso, J. G.; Lauber, C. L.; Walters, W. A.; Berg-Lyons, D.; Lozupone, C. A.;
608 Turnbaugh, P. J.; Fierer, N.; Knight, R. Global patterns of 16S rRNA diversity at a
609 depth of millions of sequences per sample. *Proc. Natl. Acad. Sci. U. S. A.* **2011**, *108*
610 *Suppl 1* (Supplement 1), 4516–4522.
- 611 (41) Edgar, R. C. UPARSE: highly accurate OTU sequences from microbial amplicon
612 reads. *Nat. Methods* **2013**, *10* (10), 996–998.
- 613 (42) Edgar, R. C. Search and clustering orders of magnitude faster than BLAST.
614 *Bioinformatics* **2010**, *26* (19), 2460–2461.
- 615 (43) Yarza, P.; Richter, M.; Peplies, J.; Euzéby, J.; Amann, R.; Schleifer, K.-H.; Ludwig, W.;
616 Glöckner, F. O.; Rosselló-Móra, R. The All-Species Living Tree project: A 16S rRNA-
617 based phylogenetic tree of all sequenced type strains. *Syst. Appl. Microbiol.* **2008**,
618 *31* (4), 241–250.
- 619 (44) Hill, M. O. Diversity and Evenness: A Unifying Notation and Its Consequences.
620 *Ecology* **1973**, *54* (2), 427–432.
- 621 (45) Jost, L. Entropy and Diversity. *Oikos* **2006**, *113* (2), 363–375.
- 622 (46) Jost, L. PARTITIONING DIVERSITY INTO INDEPENDENT ALPHA AND BETA
623 COMPONENTS. *Ecology* **2007**, *88* (10), 2427–2439.
- 624 (47) Kang, S.; Rodrigues, J. L. M.; Ng, J. P.; Gentry, T. J. Hill number as a bacterial
625 diversity measure framework with high-throughput sequence data. *Sci. Rep.*
626 **2016**, *6* (1), 38263.
- 627 (48) Santini, T. C. Application of the Rietveld refinement method for quantification of
628 mineral concentrations in bauxite residues (alumina refining tailings). *Int. J.*
629 *Miner. Process.* **2015**, *139*, 1–10.
- 630 (49) Hertel, T.; Blanpain, B.; Pontikes, Y. A Proposal for a 100% Use of Bauxite
631 Residue Towards Inorganic Polymer Mortar. *J. Sustain. Metall.* **2016**, *2* (4), 394–
632 404.
- 633 (50) Xue, S.; Zhu, F.; Kong, X.; Wu, C.; Huang, L.; Huang, N.; Hartley, W. A review of the
634 characterization and revegetation of bauxite residues (Red mud). *Environ. Sci.*
635 *Pollut. Res.* **2016**, *23* (2), 1120–1132.
- 636 (51) Ruyters, S.; Mertens, J.; Vassilieva, E.; Dehandschutter, B.; Poffijn, A.; Smolders, E.
637 The Red Mud Accident in Ajka (Hungary): Plant Toxicity and Trace Metal
638 Bioavailability in Red Mud Contaminated Soil. *Environ. Sci. Technol.* **2011**, *45* (4),
639 1616–1622.
- 640 (52) Buchman, M. F. *NOAA Screening Quick Reference Tables*; Seattle WA, 2008; Vol.

- 641 08–1.
- 642 (53) Barnes, M. C.; Addai-Mensah, J.; Gerson, A. R. The mechanism of the sodalite-to-
643 cancrinite phase transformation in synthetic spent Bayer liquor. *Microporous*
644 *Mesoporous Mater.* **1999**, *31* (3), 287–302.
- 645 (54) Xu, H.; Van Deventer, J. S. J. The geopolymerisation of aluminosilicate minerals.
646 *Int. J. Miner. Process.* **2000**, *59* (3), 247–266.
- 647 (55) Langmuir, D. *Aqueous environmental geochemistry*; Prentice Hall, 1997.
- 648 (56) Wehrli, B.; Stumm, W. Vanadyl in natural waters: Adsorption and hydrolysis
649 promote oxygenation. *Geochim. Cosmochim. Acta* **1989**, *53* (1), 69–77.
- 650 (57) Genç, H.; Tjell, J. C.; McConchie, D.; Schuiling, O. Adsorption of arsenate from water
651 using neutralized red mud. *J. Colloid Interface Sci.* **2003**, *264* (2), 327–334.
- 652 (58) Sherman, D. M.; Randall, S. R. Surface complexation of arsenic(V) to iron(III)
653 (hydr)oxides: structural mechanism from ab initio molecular geometries and
654 EXAFS spectroscopy. *Geochim. Cosmochim. Acta* **2003**, *67* (22), 4223–4230.
- 655 (59) TISDALL, J. M.; OADES, J. M. Organic matter and water-stable aggregates in soils. *J.*
656 *Soil Sci.* **1982**, *33* (2), 141–163.
- 657 (60) Six, J.; Paustian, K.; Elliott, E. T.; Combrink, C. Soil Structure and Organic Matter.
658 *Soil Sci. Soc. Am. J.* **2000**, *64* (2), 681.
- 659 (61) Six, J.; Elliott, E. T.; Paustian, K. Soil Structure and Soil Organic Matter. *Soil Sci. Soc.*
660 *Am. J.* **2000**, *64* (3), 1042.
- 661 (62) Knill, C. J.; Kennedy, J. F. Degradation of cellulose under alkaline conditions.
662 *Carbohydr. Polym.* **2003**, *51* (3), 281–300.
- 663 (63) Humphreys, P. N.; Laws, A. P.; Dawson, J. *A Review of Cellulose Degradation and the*
664 *Fate of Degradation Products Under Repository Conditions*; Nuclear
665 Decommissioning Authority (NDA), 2010.
- 666 (64) Rout, S. P.; Radford, J.; Laws, A. P.; Sweeney, F.; Elmekawy, A.; Gillie, L. J.;
667 Humphreys, P. N. Biodegradation of the alkaline cellulose degradation products
668 generated during radioactive waste disposal. *PLoS One* **2014**, *9* (9), e107433.
- 669 (65) Fuller, R. D.; Nelson, E. D. P.; Richardson, C. J. Reclamation of Red Mud (Bauxite
670 Residues) Using Alkaline-Tolerant Grasses with Organic Amendments1. *J. Environ.*
671 *Qual.* **1982**, *11* (3), 533.
- 672 (66) Wong, J. W. C.; Ho, G. Sewage sludge as organic ameliorant for revegetation of fine
673 bauxite refining residue. *Resour. Conserv. Recycl.* **1994**, *11* (1–4), 297–309.
- 674 (67) Krüger, G. Verwitterungsversuche an Leuzit. *Chemie der Erde - Geochemistry1*
675 **1939**, *12*, 236–264.
- 676 (68) Brady, P. V.; Walther, J. V. Controls on silicate dissolution rates in neutral and
677 basic pH solutions at 25°C. *Geochim. Cosmochim. Acta* **1989**, *53* (11), 2823–2830.
- 678 (69) Hamilton, J. P.; Brantley, S. L.; Pantano, C. G.; Criscenti, L. J.; Kubicki, J. D.
679 Dissolution of nepheline, jadeite and albite glasses: toward better models for
680 aluminosilicate dissolution. *Geochim. Cosmochim. Acta* **2001**, *65* (21), 3683–3702.
- 681 (70) Tole, M. P.; Lasaga, A. C.; Pantano, C.; White, W. B. The kinetics of dissolution of
682 nepheline (NaAlSi₃O₈). *Geochim. Cosmochim. Acta* **1986**, *50* (3), 379–392.
- 683 (71) Oelkers, E. H. General kinetic description of multioxide silicate mineral and glass
684 dissolution. *Geochim. Cosmochim. Acta* **2001**, *65* (21), 3703–3719.
- 685 (72) Álvarez-Ayuso, E.; Nugteren, H. W. Synthesis of dawsonite: A method to treat the
686 etching waste streams of the aluminium anodising industry. *Water Res.* **2005**, *39*
687 (10), 2096–2104.
- 688 (73) Schlesinger, W. H.; Andrews, J. A. Soil respiration and the global carbon cycle.
689 *Biogeochemistry* **2000**, *48* (1), 7–20.

- 690 (74) Zhou, J.; Bruns, M. A.; Tiedje, J. M. DNA recovery from soils of diverse composition.
691 *Appl. Environ. Microbiol.* **1996**, *62* (2), 316–322.
- 692 (75) Krishna, P.; Babu, A. G.; Reddy, M. S. Bacterial diversity of extremely alkaline
693 bauxite residue site of alumina industrial plant using culturable bacteria and
694 residue 16S rRNA gene clones. *Extremophiles* **2014**, *18* (4), 665–676.
- 695 (76) Müller, D. B.; Vogel, C.; Bai, Y.; Vorholt, J. A. The Plant Microbiota: Systems-Level
696 Insights and Perspectives. *Annu. Rev. Genet.* **2016**, *50* (1), 211–234.
- 697 (77) Bulgarelli, D.; Rott, M.; Schlaeppi, K.; Ver Loren van Themaat, E.; Ahmadinejad, N.;
698 Assenza, F.; Rauf, P.; Huetzel, B.; Reinhardt, R.; Schmelzer, E.; et al. Revealing
699 structure and assembly cues for Arabidopsis root-inhabiting bacterial microbiota.
700 *Nature* **2012**, *488* (7409), 91–95.
- 701 (78) Lundberg, D. S.; Lebeis, S. L.; Paredes, S. H.; Yourstone, S.; Gehring, J.; Malfatti, S.;
702 Tremblay, J.; Engelbrektson, A.; Kunin, V.; Rio, T. G. del; et al. Defining the core
703 Arabidopsis thaliana root microbiome. *Nature* **2012**, *488* (7409), 86–90.
- 704 (79) Jones, R. T.; Robeson, M. S.; Lauber, C. L.; Hamady, M.; Knight, R.; Fierer, N. A
705 comprehensive survey of soil acidobacterial diversity using pyrosequencing and
706 clone library analyses. *ISME J.* **2009**, *3* (4), 442–453.
- 707 (80) Liu, W.; Zhang, W.; Liu, G.; Zhang, Y.; Zhang, G. Microbial diversity in the saline-
708 alkali soil of a coastal Tamarix chinensis woodland at Bohai Bay, China. *J. Arid*
709 *Land* **2016**, *8* (2), 284–292.
- 710 (81) Huber, K. J.; Geppert, A. M.; Wanner, G.; Fösel, B. U.; Wüst, P. K.; Overmann, J. The
711 first representative of the globally widespread subdivision 6
712 Acidobacteria, *Vicinamibacter silvestris* gen. nov., sp. nov., isolated from
713 subtropical savannah soil. *Int. J. Syst. Evol. Microbiol.* **2016**, *66* (8), 2971–2979.
- 714 (82) Li, X.; Sun, M.; Zhang, H.; Xu, N.; Sun, G. Use of mulberry–soybean intercropping in
715 salt–alkali soil impacts the diversity of the soil bacterial community. *Microb.*
716 *Biotechnol.* **2016**, *9* (3), 293–304.
- 717 (83) Lage, O. M.; Bondoso, J. Bringing Planctomycetes into pure culture. *Front.*
718 *Microbiol.* **2012**, *3*, 405.
- 719 (84) Chistoserdova, L.; Jenkins, C.; Kalyuzhnaya, M. G.; Marx, C. J.; Lapidus, A.; Vorholt,
720 J. A.; Staley, J. T.; Lidstrom, M. E. The Enigmatic Planctomycetes May Hold a Key to
721 the Origins of Methanogenesis and Methylophony. *Mol. Biol. Evol.* **2004**, *21* (7),
722 1234–1241.
- 723 (85) Scheuner, C.; Tindall, B. J.; Lu, M.; Nolan, M.; Lapidus, A.; Cheng, J.-F.; Goodwin, L.;
724 Pitluck, S.; Huntemann, M.; Liolios, K.; et al. Complete genome sequence of
725 Planctomyces brasiliensis type strain (DSM 5305T), phylogenomic analysis and
726 reclassification of Planctomycetes including the descriptions of Gimesia gen. nov.,
727 Planctopirus gen. nov. and Rubinisphaera gen. nov. and emended descriptions of
728 the order Planctomycetales and the family Planctomycetaceae. *Stand. Genomic Sci.*
729 **2014**, *9* (1), 10.
- 730 (86) Ferreira, C.; Soares, A. R.; Lamosa, P.; Santos, M. A.; da Costa, M. S. Comparison of
731 the compatible solute pool of two slightly halophilic planctomycetes species,
732 Gimesia maris and Rubinisphaera brasiliensis. *Extremophiles* **2016**, *20* (6), 811–
733 820.
- 734 (87) Elshahed, M. S.; Youssef, N. H.; Luo, Q.; Najar, F. Z.; Roe, B. A.; Sisk, T. M.; Bühring,
735 S. I.; Hinrichs, K.-U.; Krumholz, L. R. Phylogenetic and metabolic diversity of
736 Planctomycetes from anaerobic, sulfide- and sulfur-rich Zodletone Spring,
737 Oklahoma. *Appl. Environ. Microbiol.* **2007**, *73* (15), 4707–4716.
- 738

739 **Figures.**



740

741

Figure 1.

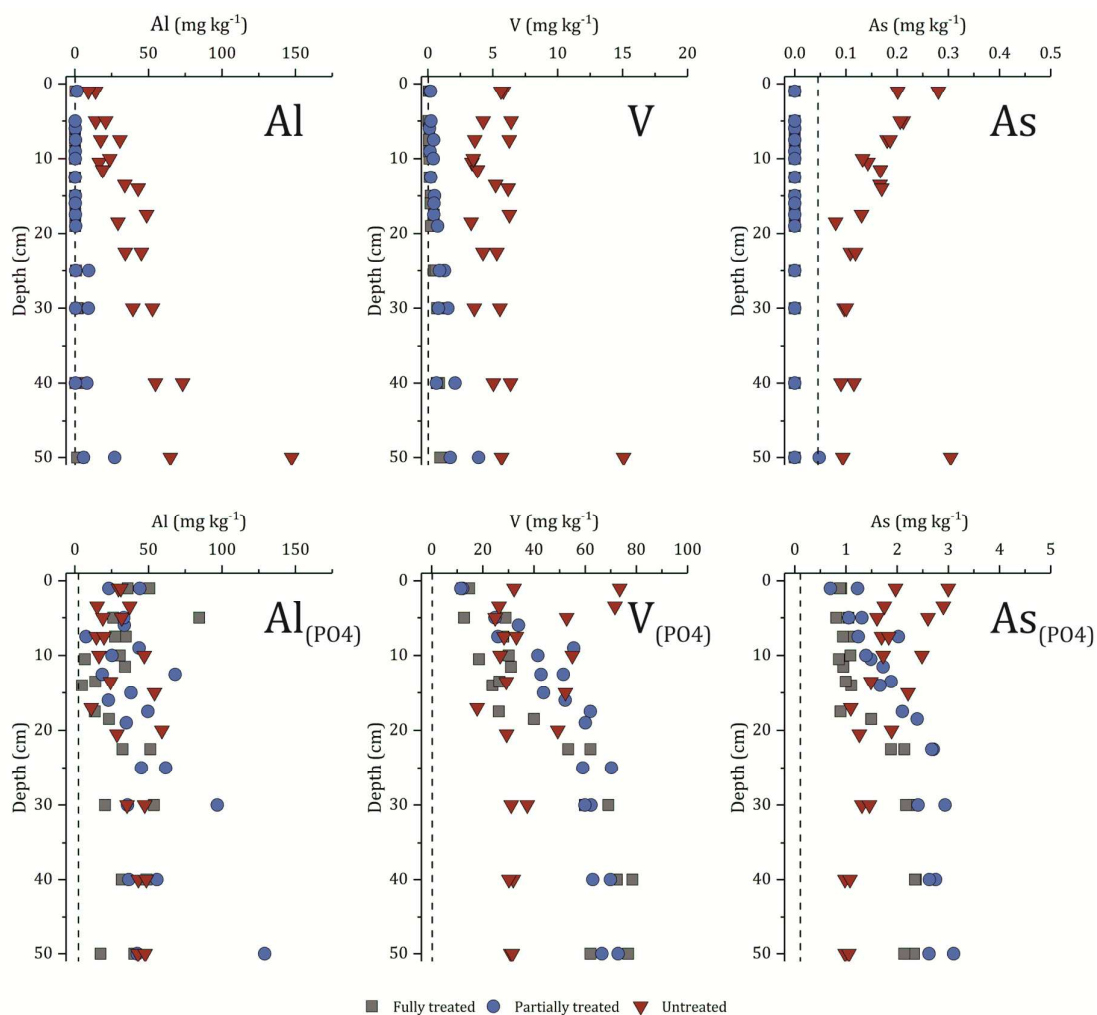
742

pH, Na, Si, and Ca aqueously extracted from fully treated, partially treated, and untreated bauxite residue as a function of depth. The dotted line represents the limit of detection for element.

743

744

745



746

747

Figure 2.

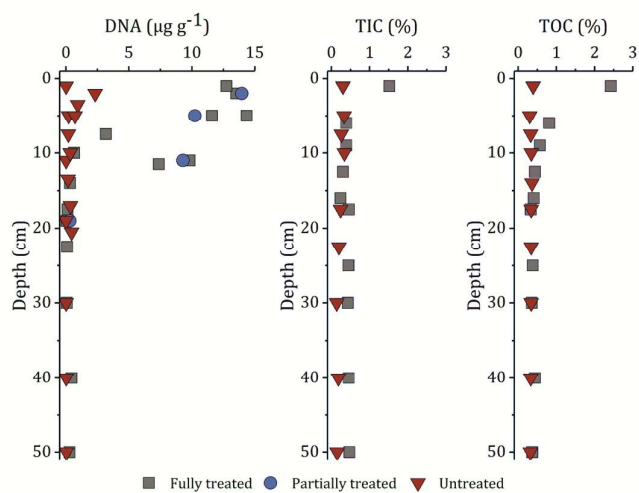
748 Concentrations of Al, V, and As in solution following aqueous and phosphate (P04)

749 extractions from fully treated, partially treated, and untreated bauxite residue as a

750 function of depth. Note the change in x-axis scale for aqueous and phosphate extracted

751 V and As. The dotted line represents the limit of detection for each element.

752



753

754

Figure 3.

755

DNA, total inorganic carbon (TIC), and total organic carbon (TOC) concentrations in

756

fully treated, partially treated, and untreated bauxite residue as a function of depth.

757

758 **Table 1.**
 759 Semi-quantitative percentage of crystalline phases present in bauxite residue as a function of treatment and average across depth, fitted
 760 using Rietveld refinement. Uncertainty on the Rietveld refinement is approximately 5 %. Full details are available in Table S2.
 761

Treatment site	Fe Oxyhydroxides		Al oxyhydroxides			Desilication Products		Ti Oxides	Other minerals
	Goethite	Hematite	Gibbsite	Boehmite	Katoite	Cancrinite	Sodalite	Perovskite	
	$\alpha\text{-FeO(OH)}$	Fe_2O_3	Al(OH)_3	$\gamma\text{-AlO(OH)}$	$\text{Ca}_3\text{Al}_2(\text{OH})_{12}$	$\text{Na}_6\text{Ca}_2\text{Al}_6\text{Si}_6\text{O}_{24}(\text{CO}_3)_2$	$\text{Na}_8\text{Al}_6\text{Si}_6\text{O}_{24}(\text{OH})_2$	CaTiO_3	
	%	%	%	%	%	%	%	%	%
Untreated	21	16	8	10	2	14	1	20	9
Fully Treated	24	19	8	7	3	10	< 0.5	20	9
Partially Treated	19	16	11	10	10	10	< 0.5	15	8

762
 763